THE DISSOLUTION RATE OF CHRYSOTILE

by

Lily Ann Hume

Thesis submitted to the Faculty of

Virginia Polytechnic Institute & State University

in partial fulfillment of the requirements of the degree of

MASTER OF SCIENCE

in

Geology

APPROVED:

J. Donald Rimstidt, Chairman

James R. Craig

Lucian W. Zelazny

May, 1991

Blacksburg, Virginia

THE DISSOLUTION RATE OF CHRYSOTILE

by

Lily Ann Hume

Committee Chairman: J. Donald Rimstidt
Geological Sciences

(ABSTRACT)

Chrysotile can be linked to three diseases: lung cancer, asbestosis, and mesothelioma. The duration and intensity of exposure along with fiber size appear to play an important role in the development of the diseases. Chrysotile is part of the serpentine group which has the general composition of $Mg_3Si_2O_5(OH)_4$. The fluids in lung tissue contain very low concentrations of magnesium and silicon. As a result they are quite undersaturated with respect to chrysotile and chrysotile will dissolve. Its persistence in lung tissue is simply a result of its dissolution kinetics. The purpose of this study was to estimate the lifetime of a respirable size fiber of chrysotile in lung tissue.

The dissolution reaction for chrysotile for pH's less than nine is:

$$Mg_3Si_2O_5(OH)_4 + 6H^+ = 3Mg^{2+} + 2H_4SiO_4 + H_2O$$

This reaction proceeds in two steps. First, the magnesium hydroxide layer of the serpentine dissolves leaving behind the silica structure of the fiber. Then the silica dissolves. Therefore, the fiber lifetime depends upon the rate of silica release. Over the range of undersaturation expected for lung tissue, the rate of silica release was found to be independent of pH with the average rate being 5.94 ($\pm$3.05) x 10^{-10} moles m^{-2} sec^{-1}. A shrinking fiber model was used to determine the relationship between dissolution time and fiber diameter. It was found that the most hazardous sized fiber of chrysotile (1 μm) would completely dissolve in about 9 months, consideration of one standard deviation above and

below the mean of the rate constant gives estimates of the lifetime of a fiber ranging from 6 to 19 months.

ACKNOWLEDGEMENTS

I would like to express many thanks to my committee chairman Don Rimstidt whose cheerfulness, patience, and guidance enabled me to complete my project. Thanks also go to committee members Jim Craig and Lucian Zelazny whose comments helped to produce a much clearer manuscript. Mark Williamson and Carl Kirby proved to be invaluable and assisted me whenever possible. The award of most reliable goes to Holly Doe, my lab assistant whose dependability allowed me to finish the project on time. I also appreciate the support of my office mates and department staff. Just one more; I would like to thank Bret Bennington for keeping me entertained and preparing all those delicious meals however, I do not want to thank him for all the weight I gained.

This research was supported in part by the Department of Interior's Mining and Mineral Resources Research Institute's Program administered by the Bureau of Mines under allotment grant G1104151 and in part by Biomedical Research Support Grant number 07095-24. Chrysotile samples were donated by Don Bloss.

TABLE OF CONTENTS

LIST OF FIGURES

LIST OF TABLES

LIST OF SYMBOLS

a	activity
d	diameter of the fiber in meters
k'	apparent rate constant (Ak)
k	rate constant
l	length
m	concentration in mol/kg
n	number of moles
r'	apparent rate of dissolution in mol kg^{-1} sec^{-1}
r	rate of dissolution in mol m^{-2} sec^{-1}
r	radius
t	time in seconds
z	aspect ratio
Q	activity quotient
A	surface area of the solid in square meters
A	lateral surface area
K	equilibrium constant
M	mass of the solution in kilograms
S	degree of saturation, Q/K
T	temperature in Kelvin
V_m	volume occupied by one mole of silica in chrysotile
V	volume

INTRODUCTION

In 1857 the use of asbestos was on the rise with the main consumer being the manufacturers of iron safes. Because of its heat resistance it was used for safe linings. At that time patents were also being requested for the development of suits for firemen (Dana, 1857). One hundred years later, asbestos was successfully being used as an stimulant to the heart muscle to increase the blood supply to the heart (Brofman, 1956). Because of its fibrous texture, tensile strength, and resistance to heat, asbestos has also found numerous commercial uses in cement pipes, brake linings, textiles, and insulation. During the last 30 years however, the beneficial aspects of asbestos have been overshadowed by an increasing awareness of the link between asbestos and lung cancer (including cancer of the trachea and bronchus), asbestosis (a fibrosis preventing normal movement of the lung), and mesothelioma (a tumor which encapsulates the lungs). Today the fear that the widespread use of asbestos has created a high risk for people who are nonoccupationally exposed has lead to a public outcry to impose regulations regarding the use of asbestos. As a result on July 12, 1989, The Environmental Protection Agency issued its latest rule (54 FR 29460) under the Toxic-Substances Control Act that prohibits the future manufacture, importation, processing, and distribution of most asbestos-containing products. The rule, which became effective August 25, 1989, is being imposed in three stages. The first stage, implemented August 1990, affected asbestos-containing felt products, flat and corrugated asbestos-containing sheet, floor tile, and asbestos clothing. The second stage to begin August 1994, will affect asbestos-containing friction products and gaskets and the third stage as of August 1996 will affect roof and nonroof coatings, paper products, friction products, and pipe. House Report 5073, the Asbestos Hazard Emergency Response Act of 1986, defines "asbestos-containing material" as any material which contains more than

one percent of the asbestiform varieties of chrysotile (serpentine), crocidolite (riebeckite), amosite (cummingtonite-grunerite), anthophyllite, tremolite, or actinolite (Table 1). The Environmental Protection Agency and other regulators have, however, been criticized because they have failed to recognize the very different physical and chemical properties of these various asbestiform minerals in their regulations.

Many authors have stated that it can be shown within reasonable doubt that all of the above minerals are linked to lung cancer (McDonald *et al.*, 1980; Meurman *et al.*, 1974; Ross, 1987; Seidman *et al.*, 1979) and asbestosis (Nicholson, 1976; Palekar, 1988; Selikoff *et al.*, 1979). However, the duration and intensity of exposure along with the mineral type and fiber size appear to play an important role in development of the diseases. Often it is difficult to pinpoint a particular mineral as the cause of lung cancer because many asbestos workers, upon whom most studies are based, have been exposed to more than one type of asbestiform mineral. Further more this problem is compounded by the fact that a majority of asbestos workers smoked tobacco products which also appear to increase the risk of lung cancer (Ross, 1987; Hammond *et al.*, 1979; Selikoff *et al.*, 1968). Harvey (1984) explains that the increase in lung cancer in asbestos workers who smoke is due to the binding of smoke-related carcinogens to the mineral fibers in the lung tissue. For asbestos workers, death due to lung cancer occurs 10 to 14 years after exposure and peaks between 30 to 35 years later (Ross, 1987).

Asbestosis, a fibrosis of the lung parenchyma caused by the inhalation of asbestos fibers, results in restricted air intake because of hardened scar tissue of the lung. The fibrosis continues to progress after inhalation of the fibers has been discontinued and eventually causes hypoxia which places a strain on the heart leading to heart failure. Asbestosis is usually diagnosed approximately 10 years after exposure and the death rate peaks 40 to 45 years later.

Table 1. Composition of serpentine and amphibole minerals.

SERPENTINE	AMPHIBOLE
Chrysotile $Mg_3Si_2O_5(OH)_4$	Riebeckite $Na_2Fe_3^{+2}Fe_2^{+3}[Si_8O_{22}](OH)_2$
Lizardite $Mg_3Si_2O_5(OH)_4$	Cummingtonite $(Mg,Fe^{+2})_7[Si_8O_{22}](OH)_2$
Antigorite $Mg_3Si_2O_5(OH)_4$	Grunerite $(Fe^{+2},Mg)_7[Si_8O_{22}](OH)_2$
	Anthophyllite $(Mg,Fe^{+2})_7[Si_8O_{22}](OH,F)_2$
	Tremolite $Ca_2(Mg,Fe^{+2})_5[Si_8O_{22}](OH,F)_2$
	Actinolite $Ca_2(Mg,Fe^{+2})_5[Si_8O_{22}](OH,F)_2$

The third disease related to asbestos is mesothelioma, a rare disease which kills approximately 1000 people per year in the United States. Mesothelioma is observed first as a thickening of the lining adjacent to the chest cavity and then the lining covering the lungs. This develops into a tumor which surrounds the lungs resulting in death approximately 20 years after exposure with the death rate continuing to rise after 45 years after exposure (Ross, 1981). In contrast to lung cancer, mesothelioma does not appear to be related to the use of tobacco products (Hammond *et al.*, 1979; Skinner, 1988; Craighead and Mossman, 1982). A study conducted by Wagner *et al.* (1960) was one of the first to link mesothelioma to asbestos. While researching mesothelioma-related deaths in South Africa where crocidolite is mined, he found that all but one patient had been in an area where exposure to crocidolite could occur. Since then a wide variety of theories relating asbestos and mesothelioma have been advanced (Selikoff, 1977; Newhouse and Berry, 1979; McDonald *et al.*, 1973). There is some controversy over which asbestiform minerals are most likely to cause mesothelioma. Mossman *et al.* (1990) has suggested that chrysotile-related mesothelioma is due to the contamination of chrysotile by amphiboles. This is based upon several studies of miners and millers who work with chrysotile and vermiculite containing tremolite, an amphibole mineral (Sebastien *et al.*, 1989; McDonald *et al.*, 1986; Churg *et al.*, 1984). Regardless, crocidolite-related mesothelioma occurs at a much higher rate than chrysotile-related mesothelioma (McDonald *et al.*, 1980; Ross, 1987, Armstrong, et al., 1984). This difference in the death rates suggests the need for additional research.

The shape, size, and durability of the fiber are important etiological factors in asbestos-related diseases. Stanton (1981) concluded that the shape of particles influenced the development of tumors in rats because rats exposed to a pulverized non-fibrous form of chrysotile and crocidolite did not develop tumors whereas, rats exposed to fibers did develop tumors. Stanton found that the degree of tumor development correlates with the

fiber dimensions. In order for asbestos-related respiratory diseases to occur, the fibers must be small enough to enter the lungs. A fiber with a diameter smaller than 5 micrometers can enter the bronchial airways and a diameter of 1.5 micrometers allows the fiber to penetrate the smaller bronchioles and the alveolar sac. Fibers longer than 10 micrometers are not easily phagocytized or engulfed by the macrophage cells. This enables the fibers to remain in the lower respiratory track or penetrate the pleural membrane and enter the interpleural space (Davis, 1981). There is some controversy over the deposition and clearance or expulsion of amphibole and chrysotile fibers in the lungs. Morgan *et al.* (1977) found that the rate of deposition and clearance for chrysotile and amphibole were similar, while Middleton et al. (1979) showed the deposition of chrysotile was much lower compared to amphibole but the clearance rates were similar. Similar deposition and clearance results have been obtained showing that the amount of amphibole deposited in the lungs of rats continues to increase as exposure time is increased. However, the amount of chrysotile deposited reaches a peak and does not continue to increase (Jones *et al.*, 1989; Wagner *et al.*, 1974). Other changes of the fibers in the lungs include longitudinal splitting along the x axis of chrysotile whereas, amphibole fibers remained unchanged (Bellman *et al.*, 1986). Amphibole fibers apparently are quite resistant to biochemical changes in the lungs. The chrysotile fibers are not as durable and tend to change morphologically and chemically. Magnesium is easily leached from chrysotile (Morgan and Holmes, 1986) and carcinogenicity and the incidence of mesotheliomas are reduced for fibers with more than 80% Mg depletion (Monchaux *et al.*, 1981). Obviously, the durability or lifetime of the fiber in the lung is an aspect well worth researching.

The mineral chosen for this study is chrysotile, a member of the serpentine group with the general composition of $Mg_3Si_2O_5(OH)_4$. The other minerals in this group are lizardite and antigorite. Chrysotile has a sheet silicate structure. The silicate layer is bonded to a

magnesium hydroxide layer. Because the interatomic dimensions of the silicate layer and magnesium hydroxide layer are different, the sheets have a tendency to curve with the silicon oxygen sheets on the inside and magnesium hydroxide sheets on the outside. A good model of chrysotile fiber structure can be found in Goni (1979). Electron-microscopic studies (Yada, 1967) perpendicular to the x axis of a chrysotile fiber clearly show the hollow nature of the fibers.

Scope of the present study

The purpose of this study is to estimate the lifetime of a respirable sized fiber of chrysotile in fluids simulating those in human lung tissue. This requires the choice of appropriate fiber size and simulation of body fluids. The fiber size considered most hazardous to the lung tissue has a diameter of <1 μm and is >10 μm long (Davis, 1981; Bellman *et al.*, 1986) . The fluids in the lung tissue contain very low concentrations of magnesium and silicon (Table 2) and are thus undersaturated with respect to chrysotile. In order to determine the amount of time needed to dissolve a respirable chrysotile fiber, a dissolution rate constant was determined and applied in a version of the shrinking particle model. There have been several previous studies of chrysotile dissolution rates (Table 3) however none of them have produced rate constants that can be used to estimate the lifetime of chrysotile in lung tissue. Most of the studies involve leaching of magnesium from the fibers. Since magnesium is easily leached leaving behind the silica framework, these studies cannot be used for the calculation of a fiber lifetime.

Solubility

Table 2 shows the concentration of Mg, SiO_2, Na, Cl, and the pH range in human plasma. Average concentrations for magnesium and silicon are 8.72×10^{-4} m and 1.48 x

Table 2. Composition range of human plasma

pH[1]	4 to 7
magnesium[2]	5.35×10^{-4} m to 1.11×10^{-3} m, avg. 8.72×10^{-4} m
silicon[2,3]	1.53×10^{-5} m to 2.81×10^{-4} m, avg. 1.48×10^{-4} m
sodium[2]	0.130 m to 0.145 m, avg. 0.138 m
chloride[2]	0.092 m to 0.121 m, avg. 0.102 m

1. Jaurand et al. (1984); 2. Iyengar et al. (1978); 3. Altman (1961)

Table 3. Summary of previous experiments measuring the rate of chrysotile dissolution

Morgan et al., 1971	Dissolution rate of radioactive labeled chrysotile *in vivo* estimated from rate of excretion of cobalt-60 to estimate the rate of magnesium leaching. 7% Mg dissolves in 1-2 days and 25-35% dissolves after 1 month.
Choi and Smith, 1972	Leaching rate of Mg^{2+} and OH^- measured for T = 5 to 45°C. Initial pH = 5.9 to 6.1, E_a (OH^- leaching) = 27.2 kJ/mole, E_a (Mg^{2+} leaching) = 22.9 kJ/mole. Initial incongruent dissolution.
Luce et al., 1972	Lizardite variety of serpentine used. T = 24°C pH = 1.53 to 9.58. Incongruent dissolution noted.
Chowdhury, 1975	T = 37°C. Initial pH = 5.9. Batch and mixed flow reactors were used. Incongruent dissolution noted.
Jaurand et al., 1977	ESCA (XPS) analysis of chrysotile fibers from human lungs and phagocytosed *in vitro* by rabbit alveolar macrophages. Showed incongruent dissolution. Magnesium removal was not constant along the axis of the fibers and varied from fiber to fiber.
Thomassin, 1977	Leaching rate of Mg^{2+} in 0.1 N oxalic acid. T = 22 to 80°C, pH = 1.5 @ 22°C. Found evidence of Mg depleted leached layer. E_a = 62.8 to 83.7 kJ/mol.
Gronow, 1987	Leaching rate in water buffered at pH 4, 7, and 9. T = 6 to 44°C. At pH 7, E_a (Mg^{2+} leaching) = 27 kJ mol^{-1} and E_a (Si leaching) = 32 kJ mol^{-1}.

10^{-4} m respectively. It will be shown that lung fluids are significantly undersaturated with respect to chrysotile, so inhaled chrysotile fibers should continuously dissolve. The dissolution reaction for chrysotile for pH's less than nine is:

$$Mg_3Si_2O_5(OH)_4 + 6H^+ = 3Mg^{2+} + 2H_4SiO_4 + H_2O \quad (1)$$

Measurement of the equilibrium constant for the above reaction

$$K = \frac{a^3_{Mg^{2+}} a^2_{H_4SiO_4}}{a^6_{H^+}} \quad (2)$$

was evaluated by Nordstrom et al., (1990) who selected the best definition of log K as:

$$\log K = 13.248 + \frac{10217.1}{T} - 6.1894 \log T \quad (3)$$

This equation predicts that the equilibrium constant for reaction (1) at body temperature (37°C) to be $10^{30.77}$. Which clearly indicates that lung fluids are significantly undersaturated with respect to chrysotile.

The silica, magnesium, and hydrogen ion concentrations measured in lung tissues are shown in Table 2. The contents of alveolar macrophage cells is comparable to an acid solution with a pH of 4 and the mesothelial cells are comparable to a pH 7 solution (Jaurand *et al.*, 1984). The average values of magnesium and silicon concentrations in blood plasma are 8.72×10^{-4} m and 1.48×10^{-4} m respectively (Iyengar *et al.*, 1978; Altman, 1961). The ionic strength (I) of plasma is about 0.12 as estimated from the average concentrations of sodium and chloride where $m_{Na^+} = 0.138$ and $m_{Cl^-} = 0.102$ (Iyengar *et al.*, 1978).

Figure 1 is a log $a_{Mg^{2+}}$ - log $a_{H_4SiO_4}$ diagram contoured in pH for 37°C. The shaded area indicates the most likely range of silica and magnesium concentrations for lung tissue. Based on this information, equilibrium of chrysotile in the lung tissue would occur

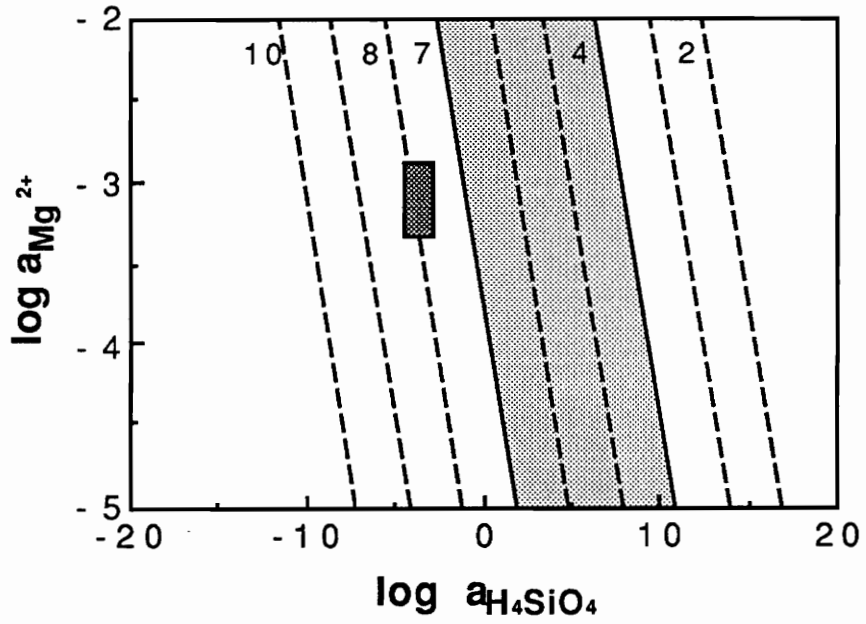

FIG. 1. Log activity Mg^{2+} vs. log activity H_4SiO_4 contoured in pH for 37°C. The shaded area to the left indicates the reported ranges of silica and magnesium concentrations for plasma. The shaded area to the right indicates the range between two cells types with pHs of 4 and 7.

approximately at pH 8. Since body fluids are constantly flushed through the system and never reach pH 8, the chrysotile in body tissues is expected to constantly dissolve.

From the equation:

$$Q = \frac{a^3_{Mg^{2+}} a^2_{H_4SiO_4}}{a^6_{H^+}} \qquad (4)$$

the activity quotient (Q) for chrysotile components in tissue can be calculated. When Q is greater than K the solution is saturated and when Q is less than K the solution is undersaturated. Based on the average values of Mg and Si found in blood plasma, Q is 1.45×10^{25} at pH 7 and 1.45×10^{7} at pH 4. The degree of saturation S = Q/K at pH 7 is 2.46×10^{-6} and at pH 4 is 2.46×10^{-24}. Thus, solutions in lung tissues are significantly undersaturated with respect to chrysotile. Chrysotile will dissolve in lung tissue and its persistence is due simply to a slow dissolution rate.

KINETICS EXPERIMENTS

Experiment design

Chrysotile, from the Bell Asbestos mine located in Quebec, Canada was cut into lengths of approximately one centimeter and ground by placing a 2.5 g sample in an acetone washed tungsten carbide shatterbox for 10 minutes. The ground solid was sized by sieving and the minus 350 micron fraction was kept for experimentation.

For experiments at pH 2, two grams of sieved solid were placed into a 500 mL flask containing a solution adjusted to the proper pH by the addition of HCl. The chrysotile particles remained suspended in the solution and approximately 25 mL of the suspension was poured into each of ten 30 mL polyethylene bottles. The bottles were placed in a constant temperature water bath set at 37° C. Each of the bottles was attached to a 20.3 cm clamp and connected to an arm extending from a Wrist-Action shaker (Fig. 2). Shaking occurred at 280 repetitions per minute and the displacement of the sample was 2.5 cm for 1/2 repetition. At specific time intervals of 10 to 180 minutes, a bottle was removed, the solution centrifuged, and the supernatant filtered using a 0.25 micron syringe filter. For experiments at pH 3, 4, and 5, 0.002 to 0.200 grams of sieved solid were placed into one liter polyethylene bottle containing 500 mL of solution which was adjusted to the proper pH by the addition of HCl. The one liter bottles were placed in a constant temperature water bath set at 37° C. Each of the bottles was attached to a 20.3 cm clamp and connected to an arm extending from a Wrist Action shaker. Shaking occurred at 240 repetitions per minute and the displacement of the sample was 2.5 cm for 1/2 repetition. At specific time intervals, a bottle was removed, a 20 mL sample obtained, centrifuged, and the supernatant filtered using a 0.25 micron syringe filter. The longest reaction time for each experiment was three hours.

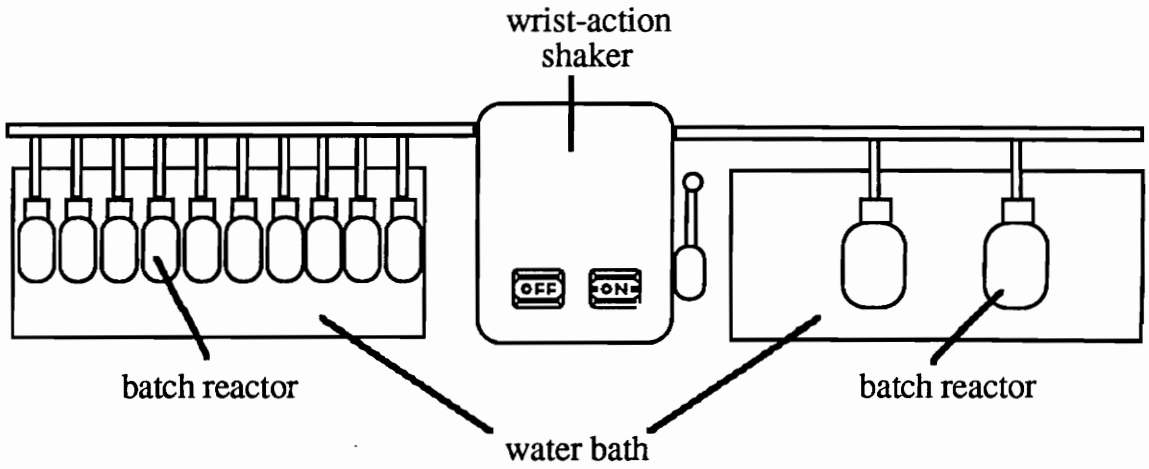

FIG. 2. Schematic diagram of the water bath design. Bottles are attached to a Wrist-Action shaker and placed in a water bath heated to 37°C.

The pH of the filtered solution was measured using a Ross combination electrode. Silica was determined using the molybdate blue method (Govett, 1961). The magnesium concentration was determined by atomic absorption spectrophotometry. The specific surface area of the solid was determined to be 33.5 $m^2\ gm^{-1}$ using a Quantachrome surface area analyzer. Scanning electron microscope (SEM) observations were also performed on the reacted and unreacted solids.

Results

Experimental results used in this study are listed in Table 4 and results which were not used are located in appendix A. NaCl added to experiments EE and HH to give an ionic strength of (0.12) near that of blood plasma did not alter the results. Apparent rates of silica release were determined for each experiment by plotting the concentration of SiO_2 in solution versus time (Fig. 3). A best fit line was drawn only through the data points which had values of Q between the range of 1.45×10^6 and 1.45×10^{26}, the ranges of values expected in lung tissue. The apparent reaction rates defined by the slopes of the lines were then normalized for each experiment using the equation:

$$r = r' / \left(\frac{A}{M}\right) \tag{5}$$

where r' is the apparent rate, A is the surface area of the solid used in the experiment in square meters, M is the mass of the solution in kilograms, and r is the rate for a system of 1 m^2/1 kg H_2O. Normalized rate data for silica release is shown in Table 5. The most general rate law for silica dissolution is:

$$r = \frac{dm_{SiO_2}}{dt} = k' m_{H^+}^b\ m_{SiO_2}^c\ m_{Mg^{2+}}^d \tag{6}$$

where $k' = Ak$. To determine the reaction order for H^+, SiO_2, and Mg^{2+}, the logarithm of both sides of equation (6) is taken giving:

$$\log r = \log k' + b \log m_{H^+} + c \log m_{SiO_2} + d \log m_{Mg^{2+}} \tag{7}$$

Table 4. Experimental results for chrysotile dissolution experiments.

SAMPLE NUMBER	ELAPSED TIME MINUTES	pH	CONCENTRATION, MOLAL SiO_2	Mg^{2+}	Q
2.00 grams chrysotile/ 0.50 kg solution					
G0	0	2.06	*3.05×10^{-5}	*4.16×10^{-5}	0.00×10^{0}
G1	10	2.76	6.39×10^{-4}	4.46×10^{-3}	7.45×10^{2}
G2	20	2.77	6.58×10^{-4}	4.50×10^{-3}	9.34×10^{2}
G3	40	2.99	7.89×10^{-4}	4.83×10^{-3}	3.48×10^{4}
G4	60	3.11	8.87×10^{-4}	5.00×10^{-3}	2.55×10^{5}
G5	80	3.44	9.85×10^{-4}	5.08×10^{-3}	3.16×10^{7}
G6	100	3.82	1.02×10^{-3}	5.17×10^{-3}	6.83×10^{9}
G7	120	4.61	1.06×10^{-3}	5.92×10^{-3}	6.08×10^{14}
G8	140	4.87	1.09×10^{-3}	5.67×10^{-3}	2.05×10^{16}
G9	160	5.25	1.15×10^{-3}	5.75×10^{-3}	4.50×10^{18}
G10	180	6.52	1.21×10^{-3}	5.75×10^{-3}	2.09×10^{26}
H0	0	2.08	*3.05×10^{-5}	0.00×10^{0}	0.00×10^{0}
H1	10	2.58	6.06×10^{-4}	3.92×10^{-3}	3.78×10^{1}
H2	20	2.71	6.39×10^{-4}	4.33×10^{-3}	3.43×10^{2}
H3	40	2.87	7.89×10^{-4}	4.50×10^{-3}	5.35×10^{3}
H4	60	3.13	8.68×10^{-4}	4.87×10^{-3}	2.98×10^{5}
H5	80	3.47	9.46×10^{-4}	4.92×10^{-3}	3.99×10^{7}
H6	100	3.94	1.02×10^{-3}	5.08×10^{-3}	3.42×10^{10}
H7	120	4.2	1.06×10^{-3}	5.29×10^{-3}	1.51×10^{12}
H8	140	6.18	1.11×10^{-3}	5.25×10^{-3}	1.22×10^{24}
H9	160	6.36	1.15×10^{-3}	5.29×10^{-3}	1.60×10^{25}
H10	180	6.93	1.38×10^{-3}	5.37×10^{-3}	6.36×10^{28}
S0	0	2.17	0.00×10^{0}	*1.25×10^{-4}	0.00×10^{0}
S1	10	2.72	4.88×10^{-4}	3.21×10^{-3}	9.34×10^{1}
S2	20	2.9	5.54×10^{-4}	3.37×10^{-3}	1.68×10^{3}
S3	40	3.28	6.60×10^{-4}	3.79×10^{-3}	6.44×10^{5}
S4	60	4.05	7.12×10^{-4}	4.33×10^{-3}	4.68×10^{10}
S5	80	5.19	8.24×10^{-4}	4.21×10^{-3}	3.97×10^{17}
S6	100	6.32	1.04×10^{-3}	4.08×10^{-3}	3.49×10^{24}
S7	120	6.48	1.15×10^{-3}	4.08×10^{-3}	3.86×10^{25}
S8	140	6.54	1.19×10^{-3}	4.17×10^{-3}	1.00×10^{26}
S9	160	6.54	1.27×10^{-3}	4.25×10^{-3}	1.23×10^{26}
S10	180	6.82	1.34×10^{-3}	4.08×10^{-3}	5.81×10^{27}

0.200 grams chrysotile/ 0.48 kg solution					
U0	0	2.91	*1.98×10^{-5}	*4.17×10^{-5}	4.66×10^{-6}
U1	10	3.35	6.30×10^{-5}	4.17×10^{-4}	2.05×10^{1}
U2	20	3.48	7.50×10^{-5}	4.58×10^{-4}	2.33×10^{2}
U3	40	3.61	9.66×10^{-5}	5.00×10^{-4}	3.03×10^{3}
U4	60	3.71	1.09×10^{-4}	7.08×10^{-4}	4.33×10^{4}
U5	80	3.8	1.21×10^{-4}	5.83×10^{-4}	1.03×10^{5}
U6	100	3.9	1.33×10^{-4}	5.83×10^{-4}	4.97×10^{5}
U7	120	4.03	1.45×10^{-4}	5.83×10^{-4}	3.56×10^{6}
U8	140	4.1	1.45×10^{-4}	5.83×10^{-4}	9.37×10^{6}
U9	160	4.21	1.45×10^{-4}	5.83×10^{-4}	4.28×10^{7}
U10	180	4.4	1.49×10^{-4}	6.25×10^{-4}	7.77×10^{8}
V0	0	2.99	0.00×10^{0}	*2.10×10^{-6}	0.00×10^{0}
V1	10	3.38	5.43×10^{-5}	2.96×10^{-4}	8.26×10^{0}
V2	20	3.45	6.87×10^{-5}	3.62×10^{-4}	6.39×10^{1}
V3	40	3.59	8.43×10^{-5}	3.75×10^{-4}	7.37×10^{2}
V4	60	3.69	9.87×10^{-5}	3.85×10^{-4}	4.37×10^{3}
V5	80	3.81	1.08×10^{-4}	4.08×10^{-4}	3.28×10^{4}
V6	100	3.9	1.15×10^{-4}	4.17×10^{-4}	1.37×10^{5}
V7	120	4.02	1.21×10^{-4}	4.31×10^{-4}	8.85×10^{5}
V8	140	4.11	1.35×10^{-4}	4.39×10^{-4}	4.00×10^{6}
V9	160	4.24	1.42×10^{-4}	4.52×10^{-4}	2.91×10^{7}
V10	180	4.4	1.48×10^{-4}	4.71×10^{-4}	3.25×10^{8}

0.250 grams chrysotile/ 0.50 kg solution					
W0	0	3.02	0.00×10^{0}	0.00×10^{0}	0.00×10^{0}
W1	10	3.75	6.49×10^{-5}	3.52×10^{-4}	3.30×10^{3}
W2	20	4.25	8.55×10^{-5}	3.77×10^{-4}	7.04×10^{6}
W3	40	5.11	1.07×10^{-4}	4.21×10^{-4}	2.20×10^{12}
W4	60	5.71	1.23×10^{-4}	4.37×10^{-4}	1.31×10^{16}
W5	80	6.68	1.40×10^{-4}	4.50×10^{-4}	1.22×10^{22}
W6	100	7.13	1.57×10^{-4}	4.67×10^{-4}	8.56×10^{24}
W7	120	7.17	1.66×10^{-4}	4.60×10^{-4}	1.60×10^{25}
W8	140	7.15	1.78×10^{-4}	4.62×10^{-4}	1.41×10^{25}
W9	160	7.21	1.85×10^{-4}	4.62×10^{-4}	3.51×10^{25}
W10	180	7.23	1.93×10^{-4}	4.69×10^{-4}	5.22×10^{25}
Y0	0	3.1	0.00×10^{0}	0.00×10^{0}	0.00×10^{0}
Y1	10	4.08	7.86×10^{-5}	3.71×10^{-4}	5.40×10^{5}
Y2	20	4.96	9.72×10^{-5}	3.98×10^{-4}	1.95×10^{11}
Y3	40	6.48	1.29×10^{-4}	4.10×10^{-4}	4.98×10^{20}
Y4	60	6.93	1.55×10^{-4}	4.12×10^{-4}	3.64×10^{23}

Y5	80	6.94	1.76×10^{-4}	4.14×10^{-4}	5.49×10^{23}
Y6	100	6.95	1.86×10^{-4}	4.12×10^{-4}	6.94×10^{23}
Y7	120	7.01	2.02×10^{-4}	4.10×10^{-4}	1.85×10^{24}
Y8	140	7.06	2.11×10^{-4}	4.17×10^{-4}	4.18×10^{24}
Y9	160	7.13	2.14×10^{-4}	4.14×10^{-4}	1.11×10^{25}
Y10	180	7.12	2.17×10^{-4}	4.04×10^{-4}	9.23×10^{24}
0.025 grams chrysotile/0.50 kg solution					
AA0	0	4.01	0.00×10^{0}	$*2.10 \times 10^{-6}$	0.00×10^{0}
AA1	10	4.09	9.79×10^{-6}	5.62×10^{-5}	3.36×10^{1}
AA2	20	4.16	1.10×10^{-5}	5.83×10^{-5}	1.25×10^{2}
AA3	40	4.18	1.47×10^{-5}	6.88×10^{-5}	4.80×10^{2}
AA4	60	4.24	1.60×10^{-5}	7.08×10^{-5}	1.41×10^{3}
AA5	80	4.38	1.98×10^{-5}	7.50×10^{-5}	1.78×10^{4}
AA6	100	4.5	1.85×10^{-5}	7.50×10^{-5}	8.18×10^{4}
AA7	120	4.94	1.98×10^{-5}	7.92×10^{-5}	4.80×10^{7}
AA8	140	4.94	2.10×10^{-5}	8.33×10^{-5}	6.33×10^{7}
AA9	160	4.87	2.23×10^{-5}	8.54×10^{-5}	2.92×10^{7}
AA10	180	4.6	2.23×10^{-5}	8.54×10^{-5}	7.00×10^{5}
0.031 grams chrysotile/ 0.50 kg solution					
BB0	0	4.17	$*1.89 \times 10^{-6}$	0.00×10^{0}	0.00×10^{0}
BB1	10	5.68	1.18×10^{-5}	4.79×10^{-5}	1.04×10^{11}
BB2	20	5.89	1.44×10^{-5}	5.41×10^{-5}	4.08×10^{12}
BB3	40	6.14	1.77×10^{-5}	6.04×10^{-5}	2.72×10^{14}
BB4	60	6.4	1.98×10^{-5}	6.46×10^{-5}	1.50×10^{16}
BB5	80	6.64	2.12×10^{-5}	6.88×10^{-5}	5.73×10^{17}
BB6	100	6.69	2.19×10^{-5}	7.08×10^{-5}	1.33×10^{18}
BB7	120	6.94	2.40×10^{-5}	7.29×10^{-5}	5.55×10^{19}
BB8	140	7	2.55×10^{-5}	7.50×10^{-5}	1.55×10^{20}
BB9	160	7.19	2.55×10^{-5}	7.50×10^{-5}	2.14×10^{21}
BB10	180	7.26	2.69×10^{-5}	7.50×10^{-5}	6.30×10^{21}
0.030 grams chrysotile/0.50 kg solution					
CC0	0	4.11	0.00×10^{0}	0.00×10^{0}	0.00×10^{0}
CC1	10	4.61	1.18×10^{-5}	5.41×10^{-5}	5.72×10^{4}
CC2	20	5.2	1.64×10^{-5}	5.83×10^{-5}	4.82×10^{8}
CC3	40	5.6	1.77×10^{-5}	6.67×10^{-5}	2.10×10^{11}
CC4	60	6.05	1.98×10^{-5}	7.29×10^{-5}	1.72×10^{14}
CC5	80	6.4	2.19×10^{-5}	7.71×10^{-5}	3.13×10^{16}
CC6	100	6.67	2.26×10^{-5}	7.92×10^{-5}	1.51×10^{18}
CC7	120	6.7	2.55×10^{-5}	7.92×10^{-5}	2.89×10^{18}
CC8	140	6.88	2.55×10^{-5}	8.12×10^{-5}	3.76×10^{19}

CC9	160	6.99	2.55×10^{-5}	8.12×10^{-5}	1.72×10^{20}
CC10	180	7.02	2.69×10^{-5}	8.33×10^{-5}	3.14×10^{20}
		0.004 grams chrysotile/0.50 kg solution			
DD0	0	5.4	*1.82×10^{-6}	0.00×10^{0}	0.00×10^{0}
DD1	10	6.1	2.49×10^{-6}	1.25×10^{-5}	2.75×10^{10}
DD2	20	6.32	3.70×10^{-6}	1.46×10^{-5}	2.00×10^{12}
DD3	40	6.77	4.91×10^{-6}	1.46×10^{-5}	1.77×10^{15}
DD4	60	7.06	3.70×10^{-6}	1.67×10^{-5}	8.25×10^{16}
DD5	80	6.82	3.70×10^{-6}	1.67×10^{-5}	3.00×10^{15}
DD6	100	7.12	3.70×10^{-6}	1.67×10^{-5}	1.89×10^{17}
DD7	120	7.14	3.10×10^{-6}	1.67×10^{-5}	1.74×10^{17}
DD8	140	7.32	4.31×10^{-6}	1.67×10^{-5}	4.06×10^{18}
DD9	160	7.17	4.91×10^{-6}	1.88×10^{-5}	9.48×10^{17}
DD10	180	7.23	5.52×10^{-6}	1.88×10^{-5}	2.74×10^{18}
		0.250 grams chrysotile/ 0.50 kg solution			
**EE0	0	3.04	*2.60×10^{-6}	0.00×10^{0}	0.00×10^{0}
EE1	10	4.03	5.83×10^{-5}	4.29×10^{-4}	2.31×10^{5}
EE2	20	4.66	6.59×10^{-5}	4.73×10^{-4}	2.38×10^{9}
EE3	40	5.52	9.37×10^{-5}	5.06×10^{-4}	8.53×10^{14}
EE4	60	6.4	1.18×10^{-4}	5.27×10^{-4}	2.88×10^{20}
EE5	80	6.53	1.55×10^{-4}	5.39×10^{-4}	3.24×10^{21}
EE6	100	6.55	1.79×10^{-4}	5.42×10^{-4}	5.75×10^{21}
EE7	120	6.61	1.92×10^{-4}	5.46×10^{-4}	1.55×10^{22}
EE8	140	6.6	2.11×10^{-4}	5.50×10^{-4}	1.67×10^{22}
EE9	160	6.61	2.20×10^{-4}	5.50×10^{-4}	2.08×10^{22}
EE10	180	6.66	2.35×10^{-4}	5.44×10^{-4}	4.59×10^{22}
		0.003 grams chrysotile/ 0.50 kg solution			
FF0	0	5.69	0.00×10^{0}	0.00×10^{0}	0.00×10^{0}
FF1	10	6.24	0.00×10^{0}	4.17×10^{-6}	0.00×10^{0}
FF2	20	6.73	0.00×10^{0}	8.33×10^{-6}	0.00×10^{0}
FF3	40	7.08	3.16×10^{-6}	1.46×10^{-5}	5.30×10^{16}
FF4	60	7.17	4.20×10^{-6}	1.67×10^{-5}	4.84×10^{17}
FF5	80	7.24	4.20×10^{-6}	1.67×10^{-5}	1.27×10^{18}
FF6	100	7.31	3.16×10^{-6}	1.87×10^{-5}	2.70×10^{18}
FF7	120	7.08	3.16×10^{-6}	1.67×10^{-5}	7.91×10^{16}
FF8	140	7.28	3.16×10^{-6}	1.87×10^{-5}	1.79×10^{18}
FF9	160	7.34	3.16×10^{-6}	1.87×10^{-5}	4.09×10^{18}
FF10	180	7.39	3.16×10^{-6}	1.87×10^{-5}	8.16×10^{18}
		0.030 grams chrysotile/0.50 kg solution			

**HH0	0	4.03	0.00×10^{0}	$*6.25 \times 10^{-6}$	0.00×10^{0}
HH1	10	4.5	8.46×10^{-6}	9.58×10^{-5}	3.57×10^{4}
HH2	20	4.73	1.12×10^{-5}	9.79×10^{-5}	1.61×10^{6}
HH3	40	4.95	1.29×10^{-5}	1.02×10^{-4}	5.04×10^{7}
HH4	60	5.17	1.46×10^{-5}	1.08×10^{-4}	1.62×10^{9}
HH5	80	5.38	1.64×10^{-5}	1.12×10^{-4}	4.13×10^{10}
HH6	100	5.52	1.76×10^{-5}	1.17×10^{-4}	3.66×10^{11}
HH7	120	5.61	1.87×10^{-5}	1.21×10^{-4}	1.61×10^{12}
HH8	140	5.74	2.00×10^{-5}	1.19×10^{-4}	1.04×10^{13}
HH9	160	5.85	2.30×10^{-5}	1.19×10^{-4}	6.36×10^{13}
HH10	180	5.92	2.30×10^{-5}	1.21×10^{-4}	1.76×10^{14}
0.002 grams chrysotile/0.50 kg solution					
II0	0	5.73	0.00×10^{0}	0.00×10^{0}	0.00×10^{0}
II1	10	6.37	4.20×10^{-6}	6.25×10^{-6}	4.06×10^{11}
II2	20	6.9	3.17×10^{-6}	4.17×10^{-6}	1.04×10^{14}
II3	40	7.02	4.20×10^{-6}	1.04×10^{-5}	1.49×10^{16}
II4	60	7.2	4.74×10^{-6}	6.25×10^{-6}	4.92×10^{16}
II5	80	7.26	4.20×10^{-6}	8.33×10^{-6}	2.10×10^{17}
II6	100	7.28	4.20×10^{-6}	1.04×10^{-5}	5.42×10^{17}
II7	120	6.72	5.23×10^{-6}	1.46×10^{-5}	1.01×10^{15}
II8	140	7.36	4.74×10^{-6}	8.33×10^{-6}	1.06×10^{18}
II9	160	7.32	5.77×10^{-6}	1.04×10^{-5}	1.78×10^{18}
II10	180	7.23	5.23×10^{-6}	6.25×10^{-6}	9.11×10^{16}

*Some of the starting solutions contained minor amounts of magnesium and silica. This did not affect the results because the release of silica is zero order with respect to hydrogen ions, magnesium, and silica.

**The solution contained 3.51 grams NaCl per 0.5 L so I = 0.12.

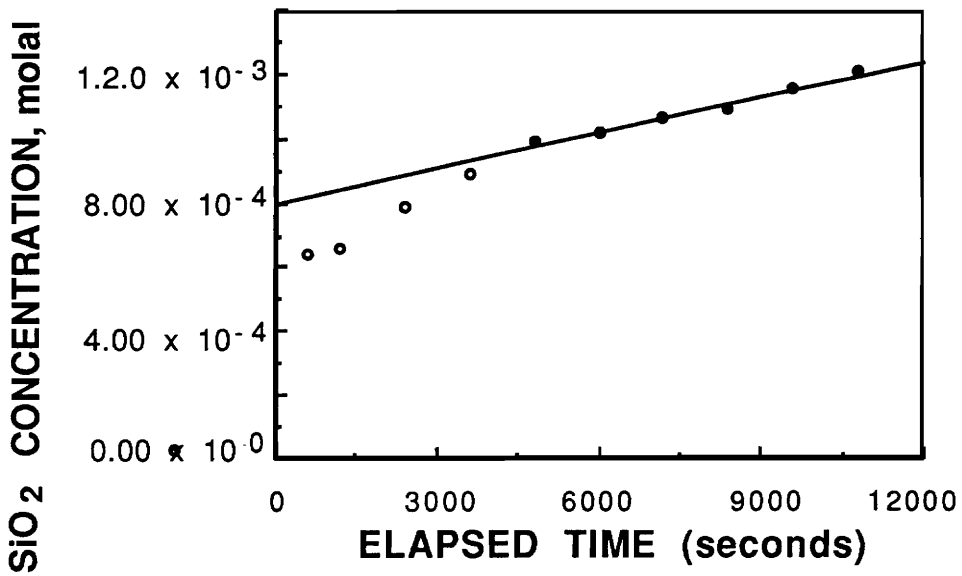

FIG. 3. Silica concentration versus time for a typical experiment (run G). The open circles were not used in this analysis because they correspond to values of Q greater than 1.45 x 10^{26} where silica dissolution rates are not zeroth order. The apparent reaction rate calculated from the slope of this line is 3.68 x 10^{-8} mol kg^{-1} sec^{-1}.

Table 5. Summary of dissolution rates for silica.

Experiment	pH	r' mol sec^{-1} kg^{-1}	A/M m^2 kg^{-1}	r mol sec^{-1} m^2	log r
G	2.06	$3.68x10^{-08}$	133.85	$2.75x10^{-10}$	-9.56
H	2.08	$4.15x10^{-08}$	133.85	$3.10x10^{-10}$	-9.51
S	2.17	$9.50x10^{-08}$	133.85	$7.10x10^{-10}$	-9.15
U	2.91	$1.00x10^{-09}$	13.94	$7.17x10^{-11}$	-10.14
V	2.99	$5.42x10^{-09}$	13.94	$3.89x10^{-10}$	-9.41
W	3.02	$1.11x10^{-08}$	16.73	$6.64x10^{-10}$	-9.18
Y	3.10	$1.21x10^{-08}$	16.73	$7.24x10^{-10}$	-9.14
*EE	3.04	$1.78x10^{-08}$	16.73	$1.07x10^{-09}$	-8.97
AA	4.01	$7.33x10^{-10}$	1.67	$4.38x10^{-10}$	-9.36
BB	4.17	$1.37x10^{-09}$	2.07	$6.60x10^{-10}$	-9.18
CC	4.11	$1.12x10^{-09}$	2.01	$5.56x10^{-10}$	-9.25
*HH	4.03	$1.26x10^{-09}$	2.01	$6.27x10^{-10}$	-9.20
DD	5.40	$1.57x10^{-10}$	0.27	$5.85x10^{-10}$	-9.23
II	5.73	$1.67x10^{-10}$	0.13	$1.24x10^{-09}$	-8.91

*solution had ionic strength (NaCl) of 0.12.

When log of the average rate versus pH data are plotted (Figure 4), a horizontal line fits the data best indicating the rate is zero order in hydrogen ions. Using the preceding technique, it can be shown that the dissolution of silica is also zero order with respect to silica and magnesium. Thus, the rate law for silica release is:

$$r = \frac{dm_{SiO_2}}{dt} = k' \, m^0_{H^+} \, m^0_{SiO_2} \, m^0_{Mg^{2+}} = k' \qquad (8)$$

The average normalized rate of silica release for 14 experiments is 5.94 ($\pm$ 3.05) x 10^{-10} moles m^{-2} sec^{-1} (error = 1σ). Because of the relationship derived in equation 8, the rate constant for this reaction is numerically equal to this rate. Magnesium release calculations are shown in appendix B.

The reacted and unreacted fibers were observed using an SEM as shown in Figure 5a (unreacted fibers) and figure 5b (fibers which were exposed to a pH 2 solution of HCl at 37°C for three hours). There are no apparent differences between the reacted and unreacted fibers when observed at this scale.

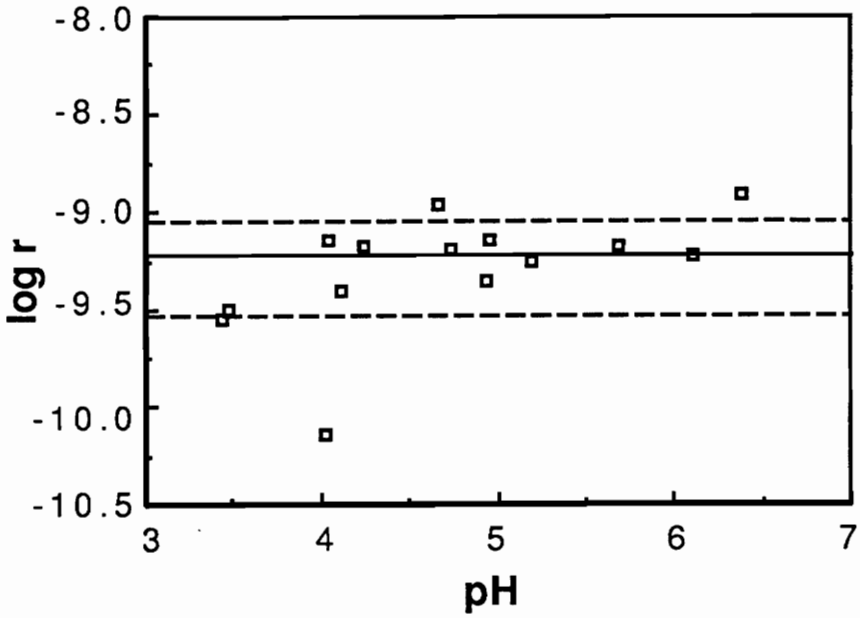

FIG. 4. The log of the mean rate of silica dissolution versus the pH of the first point used in the analysis. The solid line indicates the log mean rate and the dashed lines represents the log of one standard deviation from the mean. Silica dissolution rate is interpreted as zero order since a horizontal line fits the data well.

(a)

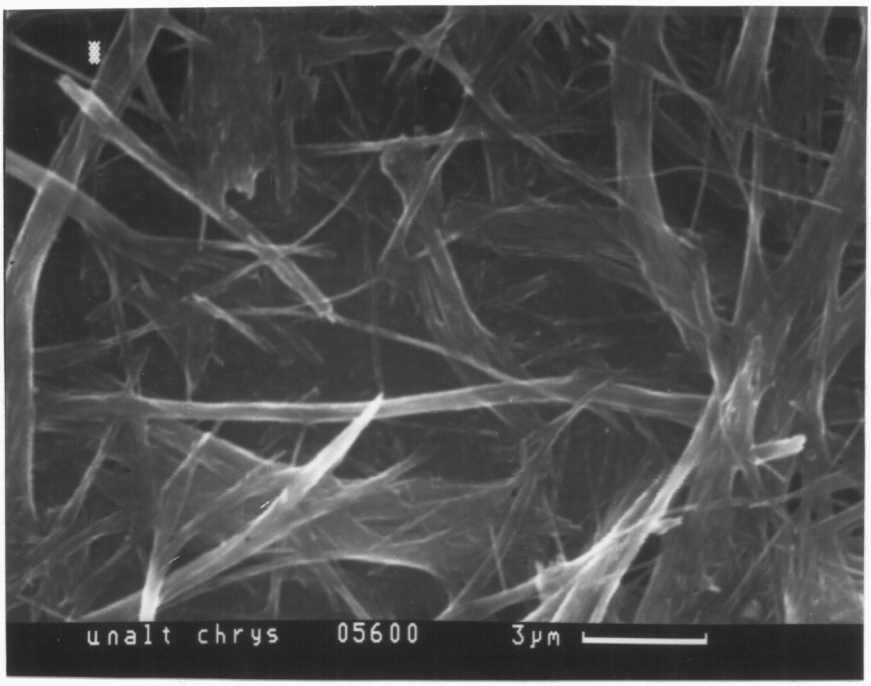

(b)

Fig. 5: Figure a shows unaltered chrysotile. Figure b shows solids remaining from an experiment which had an initial pH of 2. The exposure time was 3 hours.

DISCUSSION

Studies show that when chrysotile reacts with acid solutions, magnesium leaches out quickly leaving behind a silica structure (Morgan and Holmes, 1986). Clark and Holt (1960) were able to show incongruent dissolution of chrysotile when they found that chrysotile fibers extracted with water at 25°C resulted in a solution with small amounts of silicic acid but more than 10 times that amount of magnesium. Thus, it appears that the destruction of chrysotile fibers proceeds via two steps. First the magnesium hydroxide layer is removed by rapid leaching, then the silica layer dissolves at a slower rate. Therefore, the lifetime of a chrysotile fiber is controlled by the dissolution rate of the silica layer.

I have chosen to model the destruction of a fiber as if it were an infinitely long cylinder which is dissolving over its lateral surface. Based on this model the lifetime of a chrysotile fiber can be calculated using the equation:

$$t = \frac{3}{4}\frac{d}{V_m k} \tag{9}$$

where t is the time (sec) required for a fiber to dissolve, d is the diameter of the fiber (m), k is the rate constant (mole $m^{-2}sec^{-1}$) for silica dissolution as determined above, and V_m is the volume (m^3 mol^{-1}) occupied by one mole of silica in chrysotile as explained below. See Appendix A for the derivation of the shrinking fiber equation. The molar volume of chrysotile is 1.08×10^{-4} m^3 mol^{-1} (Robie *et al.*, 1979). Because there are two moles of silica in one mole of chrysotile, the volume occupied by one mole of silica in chrysotile is 5.4×10^{-5} m^3 mol^{-1}.

Taking the logarithm of both sides of equation (7)

$$\log t = \log\frac{3}{4} + \log d - \log V_m - \log k \tag{10}$$

gives a function which allows a comparison of fiber diameter versus dissolution time. Figure 6 shows that a chrysotile fiber with a diameter of 1 μm would dissolve completely in 9 months; consideration of one standard deviation above and below the mean of the rate constant gives estimates of the lifetime of a fiber ranging from 6 to 19 months. In comparison, a pure silica glass fiber of the same size would take 438 years based on the rate constant for amorphous silica dissolution from Rimstidt and Barnes (1980).

A rate model developed by Parry (1985) based on dissolution experiments for lizardite by Luce (1972) suggest that 30% of a 1 μm x 10 μm chrysotile fiber would dissolve in about 6 months and 100% dissolution would occur in 20 months. This value falls within 2 standard deviations of our predicted value. The differences found in dissolution rates could possibly be due to the difference in the crystal morphology between chrysotile (fibrous) and lizardite (platy). It should also be noted that Parry fitted Luce's data to a rate law which assumes that the reaction rate is proportional to Q. This assumption was not verified by our experimental data. Other serpentine dissolution studies (Morgan *et al.*, 1971; Choi and Smith, 1972) only measured the rate at which magnesium is leached from the fibers. Because magnesium is leached from chrysotile before the silica (Morgan and Holmes, 1986), these studies would yield data which are insufficient to accurately to determine the lifetime of chrysotile fibers in conditions simulating that of lung tissue.

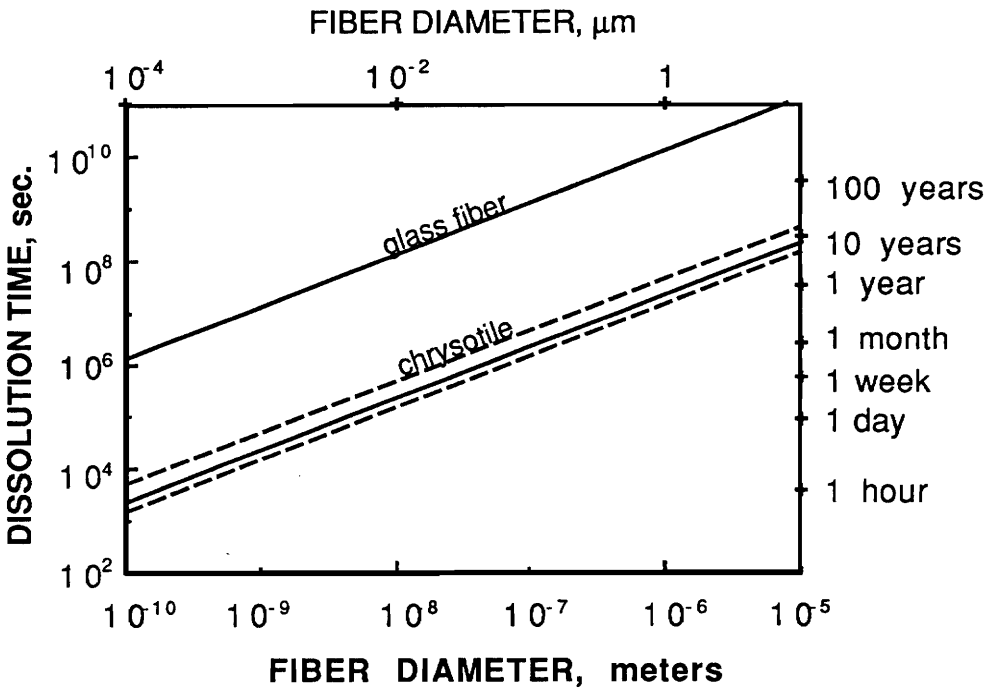

FIG. 6. Dissolution time (seconds) versus fiber diameter (meters) for chrysotile. The dashed lines indicate the predicted lifetime found by varying the silica dissolution rate constant $\pm 1\sigma$. The lifetime of glass fibers calculated using the amorphous silica dissolution rate constant of Rimstidt and Barnes (1980) is shown by the top line.

CONCLUSIONS

This research showed that because of the very low concentrations of dissolved silica and magnesium, fluids in the human body are greatly undersaturated with respect to chrysotile. The degree of saturation of chrysotile ($S = Q/K$) is estimated to range between 10^{-6} and 10^{-24}. When chrysotile fibers are exposed to solutions that are this undersaturated, the magnesium hydroxide layer is rapidly leached from them leaving behind the silica framework. This study demonstrated that for this range of undersaturation, the silica dissolves according to a simple zeroth order rate law:

$$r = Ak$$

where the rate constant is $5.94 (\pm 3.05) \times 10^{-10}$ moles m^{-2} sec^{-1}. Note that outside of this range the dissolution rate laws are different with dissolution rates slowing greatly as equilibrium is approached because of the competing precipitation reaction.

The lifetime of the most hazardous respirable-sized chrysotile fiber (1μm) can be estimated from these results using the expression

$$t = \frac{3}{4}\frac{d}{V_m k}$$

derived in Appendix A. The most probable lifetime for a 1μm diameter particle is 9 months and the longest estimated lifetime is 19 months (average + 1σ). This is a remarkably short time, although it is of the same magnitude as the estimate of Parry (1985). A fiber of silica glass of the same diameter is estimated to have a lifetime more than two orders of magnitude greater. It should also be considered that smaller fibers would dissolve in even shorter time.

These results have important implications for understanding asbestos-related diseases. On the average, death from lung cancer occurs 10 to 14 years after exposure and death due to asbestosis and mesothelioma occurs 40 and 20 years respectively after exposure. It is

observed that the time for diagnosis and death is at least an order of magnitude greater than the time for fiber dissolution. These are complicated diseases. Tumor growth develops in four stages, initiation, conversion, promotion, and malignant progression (Marks, 1989). Initiation involves gene mutation and can be related to the breakdown of foreign material in the tissue by cells which can produce carcinogens. Conversion can occur before initiation and is not well understood but appears to involve the stem cells or those cells which promote new cell growth. Promotion is simply a chronic irritation of the cells and can be caused by wounds or chemical irritants causing inflammation. The final process is malignant progression and is the growth or spreading of altered cells forming a tumor.

For the mineral chrysotile it is unclear what the cancer causing agent is, however, the damage to the lung tissue must take place soon after exposure since chrysotile dissolves fairly quickly. Therefore, it can be assumed that the chrysotile is either an initiator or a convertor and any model designed to describe disease development must explain the discrepancy between fiber lifetime to the onset of disease.

REFERENCES

Altman P. L. (1961)*Blood and Other Body Fluids* , Federation of American Societies for Experimental Biology, Washington, D. C.

Armstrong B. K., Musk A. W., Baker J. E., Hunt J. M., Newall C. C., Henzell H. R., Blundson B. S., Clarke-Hundley M. D., Woodward S. D. and Hobbs M. S. T.(1984) Epidemiology of malignant mesothelioma in western Australia. *Med. J. Aust.* **141**, 86 -88.

Bellman B., Konig H., Muhle H. and Pott F. (1986) Chemical durability of asbestos and of man-made mineral fibres in vivo. *J. Aerosol Sci.,* **17**, 341-345.

Brofman B. L. (1956) Medical evaluating of the Beck operation for coronary artery disease. *J. Am. Med. Assoc.* **162**, 1603-1606.

Choi I. and Smith R. W. (1972) Kinetic study of dissolution of asbestos fibers in water. *J. Coll. Interf. Sci* **40**, 253-261.

Chowdhury A. (1975) Kinetics of leaching of asbestos minerals at body temperature. *J. Appl Chem. Biotechnol.* **25**, 347-353.

Churg A., Wiggs B., Depaoli L., Kampe B. and Stevens B. (1984) Lung asbestos content in chrysotile workers with mesothelioma. *Am. Rev. Respir. Dis.* **130**, 1042-1045.

Clark S. G. and Holt P. F. (1960) Dissolution of chrysotile asbestos in water, acid, and alkali. *Nature (London)* **185**, 237.

Craighead J. E. and Mossman B. T. (1982) The pathogenesis of asbestos-associated diseases. *N. Engl. J. Med.* **306**, 1446-1455.

Dana J. D. (1857) *Manual of Mineralogy including Observations of Mines, Rocks, Reduction of Ores and the Applications of the Science to the Arts* , H. C. Peck and Theo. Bliss, Philadelphia.

Davis J. M. G. (1981) The biological effects of mineral fibres. *Ann. Occup. Hyg.* **24**, 227-234.

Goni J., Thomassin J. H., Jaurnad M. C., Touray J. C. (1979) Photoelectron spectroscopy analysis of asbestos dissolution in acidic media of biological interest. In *Origin and Distribution of the Elements* (L. H. Ahrens), Pergamon Press, New York.

Govett G. J. S. (1961) Critical Factors in the Colorimetric Determination of Silica. *Anal. Chim. Acta* **25**, 69-80.

Gronow J. R. (1987) The dissolution of asbestos fibres in water. *Clay Minerals* **22**, 21 -35.

Hammond E. C., Selikoff I. J. and Seidman H. (1979) Asbestos exposure, cigarette smoking and death rates. *Ann. N. Y. Acad. Sci.* **330**, 473-490.

Harvey G., Page M. and Dumas L. (1984) Binding of environmental carcinogens to asbestos and mineral fibres. *Brit. J. Ind. Med* . **44**, 396-400.

Iyengar G. V., Kollmer W. E. and Bowen H. J. M. (1978)*The Elemental Composition of Human Tissues and Body Fluids* , Verlag Chemie, New York.

Jaurand M. C., Bignon J., Sebastien P. and Goni J. (1977) Leaching of chrysotile asbestos in human lungs. *Env. Rea.* **14**, 245-254.

Jaurand M. C., Gaudichet A., Halpern S. and Bignon (1984) In vitro biodegradation of chrysotile fibres by alveolar macrophages and mesothelial cells in culture: comparison with a pH effect *Brit. J. Ind. Med.* **41**, 389-395.

Jones A. D., Vincent J. H., McIntosh C., McMillan C. H. and Addison J. (1989) The effect of fibre durability on the hazard potential of inhaled chrysotile asbestos fibres. *Exp. Pathol.* **37**, 98-102.

Luce R. W., Bartlett R. W. and Parks G. A. (1972) Dissolution kinetics of magnesium silicates. *Geochim. cosmochim. Acta* **36**, 35-50.

Marks, F. (1989) Chemical carcinogenesis, the multistage approach. *Interdisciplinary Science Reviews* 14, 233-240.

McDonald A. D., Magner D. and Eyssen G. (1973) Primary malignant mesothelial tumors in Canada 1960-1968. A pathologic review by the mesothelioma panel of the Canadian tumor reference centre. *Cancer* **31**, 869-876.

McDonald J. C., Liddell F. D. K., Gibbs G. W., Eyssen G. E. and McDonald A. D. (1980) Dust exposure and mortality in chrysotile mining, 1910-75. *Brit. J. Ind. Med.* **37**, 11-24.

McDonald J. D., McDonald A. D., Armstrong B. and Sebastien P. (1986) Cohort study of mortality of vermiculite miners exposed to tremolite. *Brit. J. Ind. Med.* **43**, 436-444.

Meurman L. O., Kiviluoto R. and Hakama M. (1974) Mortality and morbidity among the working population of anthophyllite asbestos miners in Finland. *Brit. J. Ind. Med.* **31**, 105-112.

Middleton A. P., Beckett S. T. and Davis J. M. G. (1979) Further observations on the short-term retention and clearance of asbestos by rats, using UICC reference samples. *Ann. Occup. Hyg.* **22**, 141-152.

Monchaux G., Bignon J., Jaurand M. C., Lafuma J., Sebastien P., Masse R., Hirsch A. and Goni J. (1981) Mesotheliomas in rats following inoculation with acid-leached chrysotile asbestos and other mineral fibres. *Carcinogenesis* **2**, 229-236.

Morgan A. and Holmes A. (1986) Solubility of asbestos and man-made mineral fibers in vitro and in vivo; Its significance in lung disease. *Environ. Res.* **39**, 475-484.

Morgan A., Evans J. C. and Holmes A. (1977) Deposition and clearance of inhaled fibrous minerals in the rat. Studies using radioactive tracer techniques. In *Inhaled Particles IV* (W. H. Walton), v. 1, Pergammon Press, Oxford.

Morgan A., Holmes A. and Gold C. (1971) Studies of the solubility of constituents of chrysotile asbestos in vivo using radioactive tracer techniques. *Env. Res.* **4**, 558-570.

Mossman B. T., Bignon J., Corn M., Seaton A. and Gee J. B. L. (1990) Asbestos: scientific developments and implications for public policy. *Sci.* **247**, 294-301.

Newhouse M. L. and Berry G. (1979) Patterns of mortality in asbestos factory workers in London. *Ann. N.Y. Acad. Sci.* **330**, 53-60.

Nicholson W. J. (1976) Case study 1: Asbestos__ the TLV approach. *Ann. NY Acad. Sci.* **271**, 152-169.

Palekar L. D. (1988) Effects of mineral fibers on the lung and surrounding mesothelium. In *Toxicology of the Lung* (D. E. Gardner, J. D. Crapoand E. J. Massaros D. E. Gardner, J. D. Crapoand E. J. Massaro), v. Raven Press, New York.

Parry W. T. (1985) Calculated solubility of chrysotile asbestos in physiological systems. *Env. Res.* **37**, 410-418.

Rimstidt J. D. and Barnes H. L. (1980) The kinetics of silica-water reactions. *Geochim. Cosmochim. Acta* **44**, 1683-1699.

Robie R. A., Hemingway B. S. and Fisher J. R. (1979) *Thermodynamic Properties of Minerals and Related Substances at 298.15 K and 1 Bar Pressure and at Higher Temperatures* , United States Government Printing Office, Washington.

Ross M. (1981) The geologic occurrences and health hazards of amphibole and serpentine asbestos. In *Amphiboles and Other Hydrous Pyriboles - Mineralogy* (P. H. Ribbe), v. 9A, Mineralogical Society of America, Washington

Ross M., (1987) A survey of asbestos-related disease in trades and mining occupations and in factory and mining communities as a means of predicting health risks of non occupational exposure to fibrous minerals, *American Society for Testing and Materials 83 4.*

Sebastien P., McDonald J. C., McDonald A. D., Case B. and Harley R. (1989) Respiratory cancer in chrysotile textile and mining industries: exposure inferences from lung analysis. *Brit. J. Ind. Med.* **46**, 180-187.

Seidman H., Selikoff I. J. and Hammond E. C. (1979) Short-term asbestos work exposure and long-term observation. *Ann. N. Y. Acad. Sci.* **330**, 61-89.

Selikoff I. J., (1975) Air pollution and asbestos carcinogenesis investigation of possible synergism, *Air Pollution and Cancer in Man.* IARC Scientific Publications, n. 16, 247 -253.

Selikoff I. J., Hammond E. C. and Churg J. (1968) Asbestos exposure, smoking, and neoplasia. *JAMA* **204**, 104-110.

Selikoff I. J., Hammond E. C. and Seidman H. (1979) Mortality experience of insulation workers in the United States and Canada, 1943-1976. *Ann. NY Acad. Sci.* **330**, 91-116.

Skinner H. C. W., Ross M. and Frondel C. (1988) *Asbestos and Other Fibrous Materials, Mineralogy, Crystal Chemistry, and Health Effects* , Oxford University Press, New York.

Stanton J. F., Layard M. and Tegaris A. (1981) Relation of particle dimension to carcinogenicity in amphibole asbestos and other fibrous minerals. *J. Natl. Cancer Inst.* **67**, 165-175.

Thomassin J. H., Goni J., Baillif P., Touray J. C. and Jaurand J. C. (1977) An XPS study of the dissolution kinetics of chrysotile in 0.1 N oxalic acid at different temperatures. *Phys. Chem. Minerals* **1**, 385-398.

Wagner J. C., Berry G., Skidmore J. W. and Timbrell V. (1974) The effects of the inhalation of asbestos in rats. *Br. J. Cancer* **29**, 252-269.

Wagner J. C., Sleggs C. A. and Marchand P. (1960) Diffuse pleural mesothelioma and asbestos exposure in the north western cape province. *Brit. J. Ind. Med.* **17**, 260-271.

Yada K. (1967) Study of chrysotile asbestos by a high resolution electron microscope. *Acta Cryst.* **23**, 704-707.

APPENDIX A
Unused data

The following is a list of data which was not used. Early experiments resulted in data exclusion due to a deionizing column failure where the starting solutions were contaminated with silica. A second problem encountered was the speed at which the reaction proceeded; several experimental runs were needed to adjust the solid-solution ratio. When the experiments were run at higher pHs there appeared to be fluctuations of pH due to CO_2 contamination and at this point it was not known if the reaction was dependent on pH. Finally, those experiments which did not contain ranges of Q needed for data interpretation were also excluded. It should be noted that silica and magnesium concentrations were not determined for these runs.

sample #	elapsed time	pH	sample #	elapsed time	pH
Deionizing column not functioning properly			D4	60	3.49
B0	0	2.15	D5	80	4.24
B1	15	2.69	D6	100	5.34
B2	30	2.81	D7	120	6.29
B3	60	3.12	D8	140	6.49
B4	90	3.47	D9	160	6.53
B5	120	4.41	D10	180	6.58
B6	150	5.69			
B7	180	6.23	E0	0	4.67
B8	210	6.4	E1	10	8.97
B9	240	6.17	E2	20	9.04
B10	270	6.43	E3	40	9.00
			E4	60	9.02
C0	0	2.25	E5	80	8.98
C1	10	2.63	E6	100	8.96
C2	20	2.7	E7	120	8.97
C3	40	2.82	E8	140	8.96
C4	60	2.91	E9	160	8.94
C5	80	2.98	E10	180	8.9
C6	100	3.21			
C7	120	3.11	F0	0	3.57
C8	140	3.61	F1	10	8.23
C9	160	3.89	F2	20	8.79
C10	180	3.99	F3	40	8.67
			F4	60	9.02
D0	0	2.12	F5	80	8.97
D1	10	2.63	F6	100	8.84
D2	20	2.79	F7	120	9.08
D3	40	2.98	F8	140	9.11

sample #	elapsed time	pH
F9	160	8.84
F10	180	8.82
Reaction occurred to fast.		
I0	0	4.01
I1	10	8.2
I2	20	8.51
I3	40	8.86
I4	60	8.85
I5	80	8.3
I6	100	8.57
I7	120	8.53
I8	140	8.7
I9	160	8.76
I10	180	8.56
J0	0	4.2
J1	10	8.08
J2	20	8.57
J3	40	8.45
J4	60	8.48
J5	80	8.59
J6	100	8.28
J7	120	8.1
J8	140	8.39
J9	160	8.61
J10	180	8.35
K0	0	4.18
K1	10	7.58
K2	20	8.1
K3	40	8.11
K4	60	8.04
K5	80	8.23
K6	100	8.24
K7	120	8.42
K8	140	8.44
K9	160	8.4
K10	180	8.41
L0	0	3.9
L1	10	7.49
L2	20	7.71
L3	40	7.8
L4	60	7.89
L5	80	7.87
L6	100	7.92
L7	120	7.94
L8	140	7.96
L9	160	8.09
L10	180	8.11
M0	0	4.21
M1	10	7.78
M2	20	7.84
M3	40	7.88
M4	60	7.96
M5	80	7.93
M6	100	8.17
M7	120	8.23
M8	140	8.03
M9	160	8.05
M10	180	8.21
N0	0	3.69
N1	10	7.54
N2	20	7.67
N3	40	7.75
N4	60	7.8
N5	80	7.79
N6	100	7.78
N7	120	7.88
N8	140	7.8
N9	160	7.8
N10	180	7.95
CO_2 contamination.		
O0	0	7.53
O1	10	7.83
O2	20	8.23
O3	40	8.55
O4	60	8.72
O5	80	7.91
O6	100	8.35

sample #	elapsed time	pH
O7	120	8.49
O8	140	8.5
O9	160	8.6
O10	180	8.58
P0	0	6.62
P1	10	6.8
P2	20	7.09
P3	40	6.85
P4	60	6.89
P5	80	6.95
P6	100	8.26
P7	120	8.35
P8	140	8.34
P9	160	8.1
P10	180	8.38
Q0	0	6.29
Q1	10	6.71
Q2	20	6.96
Q3	40	7
Q4	60	7.75
Q5	80	8.11
Q6	100	7.19
Q7	120	7.7
Q8	140	7.93
Q9	160	8
Q10	180	8.03
R0	0	7.8
R1	10	6.97
R2	20	7.5
R3	40	7
R4	60	7.69
R5	80	8.42
R6	100	8.25
R7	120	8.51
R8	140	8.46
R9	160	8.52
R10	180	8.28

sample #	elapsed time	pH
Reaction occurred to fast.		
T0	0	2.94
T1	10	6.88
T2	20	7.76
T3	40	7.66
T4	60	7.16
T5	80	8.18
T6	100	8.16
T7	120	8.15
T8	140	7.68
T9	160	8.04
T10	180	8.03
X0	0	4.2
X1	10	7.51
X2	20	7.77
X3	40	7.79
X4	60	7.82
X5	80	7.82
X6	100	7.84
X7	120	7.89
X8	140	7.84
X9	160	7.78
X10	180	7.79
Z0	0	4.31
Z1	10	7.73
Z2	20	7.71
Z3	40	7.86
Z4	60	7.78
Z5	80	7.78
Z6	100	7.78
Z7	120	7.81
Z8	140	7.79
Z9	160	7.74
Z10	180	7.74
Q ranges were not in the data set.		
FF0	0	5.69
FF1	10	6.24

sample #	elapsed time	pH
FF2	20	6.73
FF3	40	7.08
FF4	60	7.17
FF5	80	7.24
FF6	100	7.31
FF7	120	7.08
FF8	140	7.28
FF9	160	7.34
FF10	180	7.39
	Reaction occurred to slow.	
GG0	0	4.26
GG1	10	4.3
GG2	20	4.32
GG3	40	4.32
GG4	60	4.33
GG5	80	4.34
GG6	100	4.35
GG7	120	4.36
GG8	140	4.36
GG9	160	4.39
GG10	180	4.37

APPENDIX B
Magnesium release rate

Normalized rate data for magnesium is shown in Table 1. The effect of hydrogen ion concentration on the rate of leaching of magnesium is:

$$r = \frac{dm_{Mg^{2+}}}{dt} = k' m_{H^+}^n \quad (1)$$

To determine the reaction order for H^+, the logarithm of both sides of equation (1) is taken giving:

$$\log r = \log k' + n \log m_{H^+} \approx \log k' - n \log pH \quad (2)$$

Log rates versus pH are plotted (Figure 1); and shows a line having a slope of 0.20 ± 0.05 fits the data best with log k being equal to -9.34 ± 0.23. This indicates the reaction order is 0.20 with respect to hydrogen and can be written as:

$$r = k' [H^+]^{0.20} \quad (3)$$

These results are comparable to the results of Bales (1985) who found that the reaction order with respect to hydrogen ion concentration is 0.24.

Table 1. Summary of dissolution rates for magnesium.

Experiment	pH	r' mol sec^{-1} kg^{-1}	A/M m^2 kg^{-1}	r mol sec^{-1} m^{-2}	log r
G	2.76	2.45×10^{-07}	133.85	1.83×10^{-09}	-8.74
H	2.58	3.05×10^{-07}	133.85	2.28×10^{-09}	-8.64
S	2.72	3.20×10^{-07}	133.85	2.39×10^{-09}	-8.62
U	3.35	5.58×10^{-08}	13.94	4.00×10^{-09}	-8.40
V	3.38	2.42×10^{-08}	13.94	1.73×10^{-09}	-8.76
W	3.75	3.12×10^{-08}	16.73	1.86×10^{-09}	-8.73
Y	3.1	1.20×10^{-08}	16.73	7.19×10^{-10}	-9.14
*EE	4.03	3.25×10^{-08}	16.73	1.94×10^{-09}	-8.71
AA	4.09	5.23×10^{-09}	1.67	3.13×10^{-09}	-8.50
BB	5.68	6.30×10^{-09}	2.07	3.04×10^{-09}	-8.52
CC	4.61	7.00×10^{-09}	2.01	3.49×10^{-09}	-8.46
*HH	4.5	5.90×10^{-09}	2.01	2.94×10^{-09}	-8.53
DD	6.1	8.27×10^{-10}	0.27	3.09×10^{-09}	-8.51
II	6.37	2.15×10^{-09}	0.13	1.61×10^{-08}	-7.79
FF	6.24	3.87×10^{-09}	0.20	1.93×10^{-08}	-7.71

*solution had ionic strength (NaCl) of 0.12.

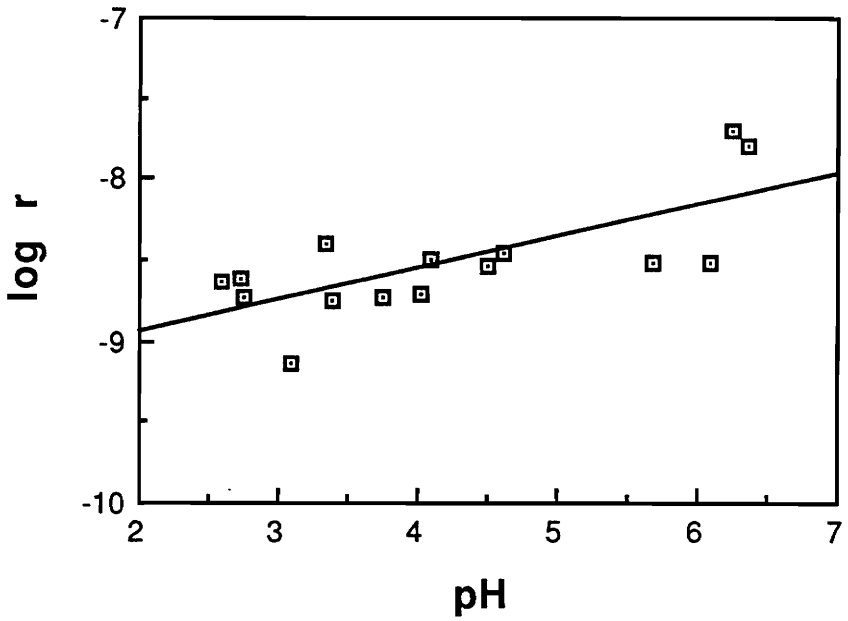

FIG. 1. The log of the rates of magnesium dissolution versus the pH. Magnesium dissolution rate is interpreted as having a reaction order of 0.20 with respect to hydrogen. The best fit line is described by log r = (0.20 (±0.05))(-log pH) - 9.34 (±0.23).

APPENDIX C

Derivation of the shrinking fiber model
by J. Donald Rimstidt

The lateral surface area (A) of a cylinder is given by

$$A = 2\pi rl \tag{1}$$

and its volume (V) is given by

$$V = \pi r^2 l \tag{2}$$

where r is the radius of the cylinder and l is its length. The aspect ratio (z) of the cylinder is defined as

$$z = \frac{r}{l} \tag{3}$$

so that

$$r = lz \tag{4}$$

and equations (1) and (2) can be recast as

$$A = 2\pi l^2 z \tag{5}$$

and

$$V = \frac{\pi r^3}{z} \tag{6}$$

Equations (5) and (6) can be substituted into the general relationship between the surface area of a solid and its volume

$$A = bV^{2/3} \tag{7}$$

to determine that

$$b = 2\frac{\pi^{1/3}}{z^{1/3}} \tag{8}$$

Furthermore, the volume of material (V) can be defined as

$$V = nV_m \tag{9}$$

where n is the number of moles of substance in the cylinder and V_m is its molar volume. Equations (7), (8), and (9) can be combined to give

$$A = 2\frac{\pi^{1/3} V_m^{2/3} n^{2/3}}{z^{1/3}} \tag{10}$$

The rate measurements show that the rate of silica release from the fibers is given by the rate law

$$\frac{dn}{dt} = -Ak \tag{11}$$

and when (10) is substituted into (11) the rate law becomes

$$\frac{dn}{dt} = -2\frac{\pi^{1/3} V_m^{2/3} k n^{2/3}}{z^{1/3}} \tag{12}$$

which can be integrated

$$\int_n^0 \frac{1}{n^{2/3}} dn = -2\frac{\pi^{1/3} V_m^{2/3} k}{z^{1/3}} \int_0^t dt \tag{13}$$

to give

$$-3n^{1/3} = -2\frac{\pi^{1/3} V_m^{2/3} k t}{z^{1/3}} . \tag{14}$$

Equation (14) can be rearranged to

$$t = \frac{3}{2}\frac{n^{1/3} z^{1/3}}{\pi^{1/3} V_m^{2/3} k} \tag{15}$$

and the definitions of n, from equation (9) and z, from equation (3), are substituted into (15) to give

$$t = \frac{3}{2}\frac{r}{V_m k} . \tag{16}$$

which gives the time to dissolve a fiber of radius r. This equation can be made somewhat more compatible with current practice of defining particle dimensions by realizing that

$$r = \frac{d}{2} \tag{17}$$

so (16) can be rewritten in terms of the diameter of the fiber to give

$$t = \frac{3}{4}\frac{d}{V_m k} . \tag{18}$$

VITA

Lily Ann Hume was born on January 15, 1961 in Nashville, Tennessee and as a child moved with her parents to Bowling Green, Kentucky where she graduated from Bowling Green High School in 1979. After spending several years of living life to its fullest, she returned to school and earned a Bachelor of Science Degree in Geology from Western Kentucky University in 1989. The author then entered Virginia Polytechnic Institute and State University located in Blacksburg, Virginia, and she obtained her Master of Science Degree in Geology in June of 1991. She intends to relocate in Lafayette, Louisiana where she will be employed by Union Oil of California.